Kyba, C., Ruby, A., Kuechly, H., Kinzey, B., Miller, N., Sanders, J., Barentine, J., Kleinodt, R., Espey, B. (2020 online): Direct measurement of the contribution of street lighting to satellite observations of nighttime light emissions from urban areas. - Lighting Research & Technology.

https://doi.org/10.1177/1477153520958463

Lighting Res. Technol.
XX(X):1–17

DOI: 10.1177/ToBeAssigned
www.sagepub.com/
SAGE

Direct measurement of the contribution of street lighting to satellite observations of nighttime light emissions from urban areas

CCM Kyba PhD[a,b], A Ruby BSc[a,c], HU Kuechly Dipl-Geoökol[a], B Kinzey MS[d], N Miller MS[d], J Sanders MBA[e], J Barentine PhD[f,g], R Kleinodt Dipl-Ing[h], B Espey PhD[i]

Received 19 March 2020; Revised 21 July 2020; Accepted

Abstract

Nighttime light emissions are increasing in most countries worldwide, but which types of lighting are responsible for the increase remains unknown. Also unknown is what fraction of outdoor light emissions and associated energy use are due to public light sources (i.e. streetlights) or various types of private light sources (e.g. advertising). Here we show that it is possible to measure the contribution of street lighting to nighttime satellite imagery using "smart city" lighting infrastructure. The city of Tucson, USA, intentionally altered its streetlight output over 10 days, and we examined the change in emissions observed by satellite. We find that streetlights operated by the city are responsible for only 13% of the total radiance (in the 500-900 nm band) observed from Tucson from space after midnight (95% confidence interval 10-16%). If Tucson did not dim their streetlights after midnight, the contribution would be 18% (95% confidence interval 15-23%). When streetlights operated by other actors are included, the best estimates rise to 16% and 21% respectively. Existing energy and lighting policy related to the sustainability of outdoor light use has mainly focused on street lighting. These results suggest an urgent need for consideration of other types of light sources in outdoor lighting policy.

[a]GFZ German Research Centre for Geosciences, Telegrafenberg, 14473 Potsdam, Germany
[b]Leibniz-Institute of Freshwater Ecology and Inland Fisheries, Müggelseedamm 310, 12587 Berlin, Germany
[c]Eberhard Karls Universität Tübingen, 72074 Tübingen, Germany
[d]Pacific Northwest National Laboratory, Portland, OR 97204, USA
[e]City of Tucson, Tucson, AZ 85701, USA
[f]International Dark-Sky Association, Tucson, AZ 85719, USA
[g]Consortium for Dark Sky Studies, University of Utah, Salt Lake City, UT 84112, USA
[h]KD Elektroniksysteme GmbH, 39261 Zerbst, Germany
[i]Trinity College Dublin, College Green, Dublin, 2, Ireland

Corresponding author:
Christopher Kyba, GFZ German Research Centre for Geosciences, Telegrafenberg, 14473 Potsdam, Germany
Email: kyba@gfz-potsdam.de

1 Introduction

Nighttime outdoor light emissions are increasing in most countries worldwide.[1,2] As a result, much of the world is now light polluted,[3] with consequences for many species and whole ecosystems.[4,5,6,7] Sustainability policy related to outdoor lighting has focused mainly on energy consumption of street lighting (e.g. the European Ecodesign directives[8]), but the observed increases in light emission calls the efficacy of such approaches into question. Efforts to reduce light pollution through lighting policy at regional or national scale are increasingly common, but are not yet widespread.[9,10,11,12] These efforts would be most effective if targeted at the sources that produce the greatest emissions. Unfortunately, which types of lighting are responsible for current increases and the contributions of public (e.g. streetlights) relative to private light sources (e.g. advertising, sports lighting) are both unknown. The aim of this paper is to demonstrate that "smart city" lighting infrastructure makes it possible to remotely sense the contribution of street lighting to the upward emissions of light observed from space.[13,14] (Note to readers: for the sake of readability, we sometimes use "light" to refer to electromagnetic radiation in the ultraviolet, visible, and near-infrared range. In cases where confusion could arise, we are more precise with our wording.)

The relative contribution of different light sources to overall urban illumination has been examined only indirectly in the past, in only a small number of places, and with variable results. The total upward light emission fraction from roadway lighting in Flagstaff, Arizona, USA was estimated to be 12%, based on a lighting inventory.[15] Aerial photography of Berlin, Germany, revealed that light from "street areas" was responsible for 32% of the near-zenith-directed light,[16] although this total includes emissions from sources such as illuminated advertisements or facades, and automobile headlights. Other researchers have estimated the contribution of upward directed light by observing changes in artificial skyglow. During the Second World War,[17] the contribution of streetlights to sky brightness was experimentally measured to be 53% for one city, and estimated to be 33% for an "average city". Similar contributions of 50% and 33% were estimated for Reykjavik in 2006[18] and for Vienna in 2017,[19] but a dramatically different estimate was recently published for Galicia, Spain: 80% contribution in the early evening, rising to nearly 100% late at night.[20] This overall inconsistency, and the fact that nearly all of the studies predate solid state lighting, motivated us to devise an experiment using "smart city" lighting infrastructure that would both yield an unambiguous result and provide information for the first time about how the contribution of emissions due to street lighting varies across a city.

In 2017, the city of Tucson, USA, converted its streetlights from high pressure sodium bulbs to 3000 Kelvin "white" LEDs. During this conversion, they reduced the total lumen output[21] from 445 Mlm to 142 Mlm. The city also installed a control system to dim their streetlights and provide near-real-time lamp-by-lamp electrical power consumption reporting. This "smart city" infrastructure makes it possible to measure the relative contribution of street light to total light emissions, by experimentally varying the light output of the city. In this paper, we report on the results of such an experiment, undertaken during 29 March to 7 April 2019 and examining electromagnetic emissions in the 500-900 nm range.

The methods and results presented here show that it is possible to remotely sense the fraction of emissions that come from streetlights, and measure the relationship between lamp lumen output and radiance detected from space. Readers should keep in mind that the relative contribution of streetlights to energy consumption for outdoor light, skyglow, or other environmental impacts is not the same as the fraction visible from space. For example, the position and emission direction are of particular importance for environmental impact: the direct illumination of a water body will have much more of an impact on flora and fauna than the same number of lumens directed at a concrete parking lot. The specrum can also play a role, as short wavelength light both produces more skyglow[22] and has a greater impact on many species.[23]

Nevertheless, this work does move us closer towards an eventual goal of being able to remotely sense the energy consumption for all types of outdoor lighting. This ability would greatly assist in evaluating the effectiveness of sustainability policy related to light use. We hope that improved understanding of the contribution of different sources to night lights data will also benefit researchers using nighttime lights across diverse fields.[24,13,14]

2 Methods

Dimming experiment

The experiment was carried out in the city of Tucson, Arizona, USA (Fig. 1). The city has a complete inventory of 19,546 streetlights tagged with geographical coordinates (Fig. 2), and can adjust the power of each lamp individually using a lighting control system. The city also has an inventory of streetlights that are not operated by the city, which was created during an audit before the conversion to LED. These 2,998 additional streetlights are mainly high pressure sodium (HPS) lights, and are estimated to consume 356 kW of electrical power (Fig. 2).

In order to save energy and prolong the operational life of their streetlights, nearly all of the streetlights operated by the city of Tucson are set to only 90% of rated electrical power during the bright phases. Each night at midnight, most streetlights in the city are dimmed from 90% to 60% (exceptions include streetlights at intersections or pedestrian crosswalks). A small number of lights are dimmed at 3:00 instead of midnight. The total power consumption of the city's streetlight network on a usual night is thus 1.46 MW before midnight, 1.08 MW between midnight and 3:00, and 1.07 MW from 3:00 until the lights are turned off in the morning.

The altered dimming regime began at midnight (local time, UTC-7) on the morning of March 29, 2019. During this period, most streetlights that are normally dimmed to 60% were instructed to instead dim to 30%. To allay concerns about safety, lights at intersections and crosswalks were instructed to remain at 90% as on a standard night. The same dimming schedule

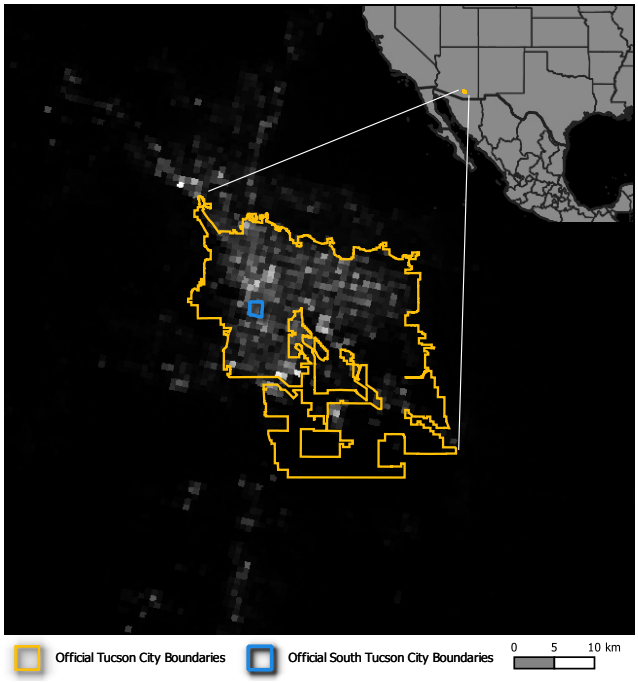

Figure 1. Tucson city limits. The inset at top right shows where Tucson is located, in the southwestern USA (Background map GADM version 3.4, 2018). The main image shows the city limits of Tucson and South Tucson (an independent municipality that has its own streetlights, and did not take part in the experiment). The background image is the DNB image from the night of 3 April 2019 (see "Satellite data and processing" below.) Colour version of this and other figures are available online.

was applied for the five following evenings: 90% before midnight, and 30% after midnight. On the evening of April 3, nearly all city of Tucson streetlights were set to run at 100% for the entire night, and this configuration applied for the mornings of April 4-7. On the evening of April 7, the test was ended, and the standard city dimming schedule was applied from April 8 onward (i.e. 90% before midnight and 60% after midnight). The city did not receive any comments from residents regarding the test, which is not surprising given the late hour and the fact that no lights were turned off (see e.g. Green et al.[25]).

The original intent was to run 5 nights each in both the bright and dimmed condition, but for an unknown reason, the dimming system did not issue the brightening command as planned on the evening of April 2. The city's lighting system allows the operator to query the streetlights regarding which setting was applied on any night of the past 3 months. This lamp-by-lamp dataset was recorded during and after the experiment, and is available upon request. We used these tables to determine the total electrical power consumption of the city lighting system (Tab. 1). For a relatively small fraction of streetlights, these instructions may not have been properly received, or were not acted on, as their records of setting on the nights in question show them to have not dimmed to the instructed value. These were examined after the experiment, and several different failure modes were found to be responsible, ranging from firmwear issues to improper wiring from the factory. As a result, each night of the experiment did not have identical light output. The revised dimming commands were re-sent each night, and it appears that the number of streetlights being correctly set increased from night to night (Tab. 1).

On most nights, about 5% of the city streetlights consistently report no power consumption (Fig. 2, Tab. 2). We believe that in most cases, the lights were on during these nights and operating at 100% illumination, but did not report their consumption due to communication issues. However, since we cannot know whether any individual lamp reported correctly or not, all streetlights reporting zero power are ignored in the analysis (i.e. assumed to be off). In addition to the full city analysis, individual hexagonal regions with 10 km^2 area were established and examined. Within these hexagons, the fraction of lamps reporting no power consumption varied slightly, however from night to night the fraction of streetlights reporting no power consumption within each individual hexagon stayed the same to within 4% over the six nights of the analysis. The one exception is that for two of these regions, there was a larger downward fluctuation on the morning of March 29 (Tab. 2). For this reason, the data from that morning was not included in the fits in those two regions (unfilled markers in Fig. 11).

In response to a reviewer's request, after performing the experiment we examined the linearity of a selection of 13 streetlights on a major street during several nights of June 2020. Each night, the lights were set to dim to different levels, and the next day the reported Wattage was checked. The following night, the illuminance was measured the next night at a point on the curb closest to the pole, using a calibrated Minolta CL 200A. Stray light from lamps across the street was blocked with a clipboard. On the night of 24-25 June, the measurement was done with the lights in the standard setting before (90%) and after (60%) midnight. One lamp did not change illuminance throughout, and was discarded from the test. The results for the other lamps are summarized in Table 3.

The illuminance at the curb varied by a surprising amount, from 1.5-9.3 lux on the 100% night (these differences were visible by eye). Comparing the illuminance for each lamp to its value on the 100% night showed that the visible band light output of the group of 12 streetlights is nearly proportional to the set power (and the reported electrical power consumption).

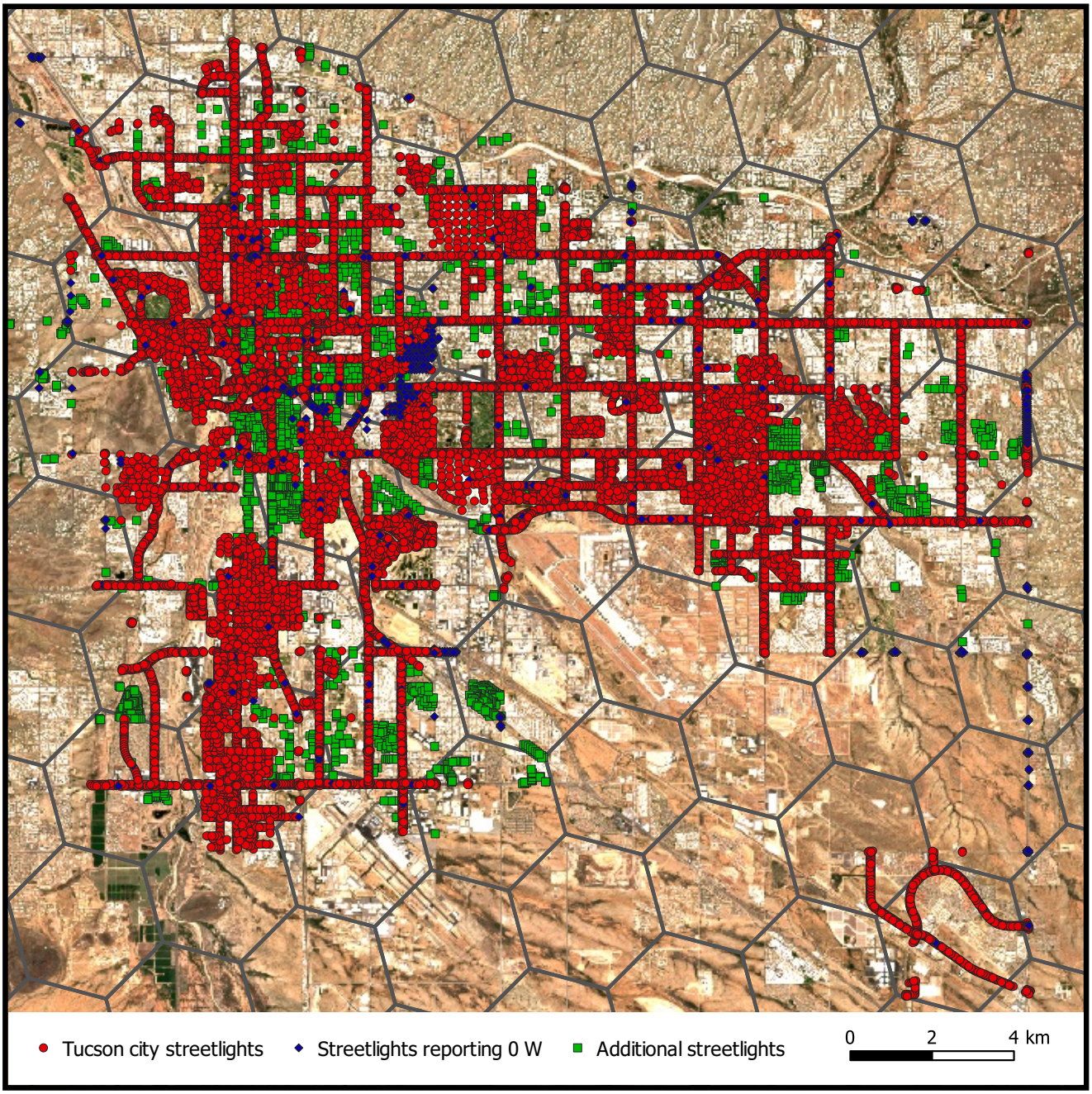

Figure 2. Map of location of the 19,546 streetlights operated by the city of Tucson, and 2,998 known streetlights operated by other entities (background image from Sentinel 2, produced from ESA remote sensing data). In the online version, the lights are colour coded according to their reporting status on 28 March 2019. 18,172 streetlights (red, 93%) correctly reported their settings, while 1,374 streetlights (blue) incorrectly reported zero power consumption. The streetlights that are not operated by the city are shown in green. The background hexagons show the analysis regions described later in the methods.

We additionally examined a separate set of 23 streetlights in a residential area on the night of 23-24 June (before and after midnight). These results were similar to the test area (median for the 60% setting was 61% of the inferred 100% value). We are therefore confident that the fractional change in luminous flux from the streetlights is proportional to the electrical power the lights reported consuming.

Satellite data and processing

Data on emissions of electromagnetic radiation in the 500-900 nm range were obtained from the Suomi NPP Visible Infrared Imaging Radiometer Suite Day/Night Band (DNB). These data have a spatial resolution of approximately 750 meters across the entire swath, with a geolocation uncertainty of 266 m (nadir) to 1151 m (edge of scan).[26] The satellite orbits the Earth 14 times per day in a polar orbit with a 16 day repeat window. At Tucson's latitude, there are one or two passes each night which include Tucson in the swath. The overpasses used in the analysis took place between 1:41 to 2:56 local time (Tab. 4).

Table 1. Total electrical power consumption for LED streetlights in Tucson. The first row shows the nominal settings (i.e. what the lights are instructed to do on a regular night). The remaining lines show the power draw reported back from the streetlights on the specified nights. "Power early" refers to power before midnight (the evening one calendar day earlier), "power late" refers to power after midnight. Analysis was only undertaken during the 6 clear nights. Note that there were two satellite overpasses on 7 April 2019, and only the second was cloud-free (indicated by *).

Date (UTC)	Condition	Power early (kW)	Power late (kW)	Weather
nominal	standard	1457	1065	
28 March 2019	standard	1337	974	cloudy
29 March 2019	dim	1340	702	clear
30 March 2019	dim	1350	690	cloudy
31 March 2019	dim	1355	683	clear
1 April 2019	dim	1360	674	cloudy
2 April 2019	dim	1360	671	cloudy
3 April 2019	dim	1410	672	clear
4 April 2019	bright	1492	1286	cloudy
5 April 2019	bright	1494	1414	cloudy
6 April 2019	bright	1496	1431	cloudy
7 April 2019*	bright	1500	1384	clear
8 April 2019	standard	1413	1066	clear
9 April 2019	standard	1374	1025	cloudy
10 April 2019	standard	1375	1014	cloudy
11 April 2019	standard	1363	1010	clear

Table 2. Number of streetlights reporting power consumption by date for the six hexagons included in Fig. 11. "C" stands for "central" and "CTB" stands for "central & tall buildings". The four suburban hexagons are listed in order from northeast to southwest. The top row shows the total number of streetlights located within the hexagon, the following lines show how many reported power consumption on each of the nights

Date (UTC)	C	CTB	Suburban 1	Suburban 2	Suburban 3	Suburban 4
nominal	1108	1127	140	265	113	405
29 March 2019	851	1046	126	229	99	395
31 March 2019	943	1081	127	234	99	395
3 April 2019	977	1082	127	234	99	394
7 April 2019	992	1084	126	234	99	393
8 April 2019	977	1084	126	232	99	393
11 April 2019	941	1092	127	236	99	394

Table 3. Test of the dimming linearity. For each lamp, the fractional illuminance was calculated (relative to the night the lamp was set to 100%), and the group median, mean, and sample standard deviation are shown.

Setting	Median	Mean $\pm$ standard deviation
100%	6.8 lux	5.9 $\pm$3.2 lux
90%	92%	92$\pm$4%
60%	63%	63.3$\pm$2%
30%	31%	32$\pm$3%

Table 4. Satellite acquisition and correction parameters. The zero offset ($S_{0,i}$) and multiplicative offset correction factor (g_i) are defined in the text.

Date (UTC)	Local time	Nadir angle	Zero offset	Multiplicative offset
29 March 2019	2:25	21.9	1.75	0.961
31 March 2019	1:47	32.2	2.40	0.990
3 April 2019	2:31	29.5	2.59	0.993
7 April 2019	2:56	48.8	4.30	1.087
8 April 2019	2:37	35.9	3.02	0.989
11 April 2019	1:41	38.4	1.64	1.024

Data were downloaded from the NOAA CLASS server (www.class.noaa.gov). Environmental Data Records were used to select the overpasses used in the analysis. Specifically, images of the "Cloud Cover Layers" product were inspected for cloud cover in the Tucson region, and overpasses with cloud cover were rejected. Six overpasses were determined to have clear skies in the study region (Tab. 1). For these six nights, DNB data from the Sensor Data Records were analyzed further. The positions and orientations of the individual pixels are not identical each night (Fig. 3B,C). The data for the Tucson region were clipped and then reprojected onto a 50 meter equal area grid (EPSG:32612) using nearest neighbor sampling, to allow us to work with raster data. Despite the altered orientation and position of the individual pixels, the dimming in the region contained within the solid blue rectangle in Fig. 3B,C is clearly visible. The area enclosed by the dashed rectangle contains few streetlights, and looks quite similar between the two images.

The two blue rectangles in Fig. 3 demonstrate the potential danger that spatial aliasing could pose to an analysis, due to the grid layout of Tucson (large streets occur at 1 mile intervals). The dashed rectangle contains only 39 streetlights. However, if

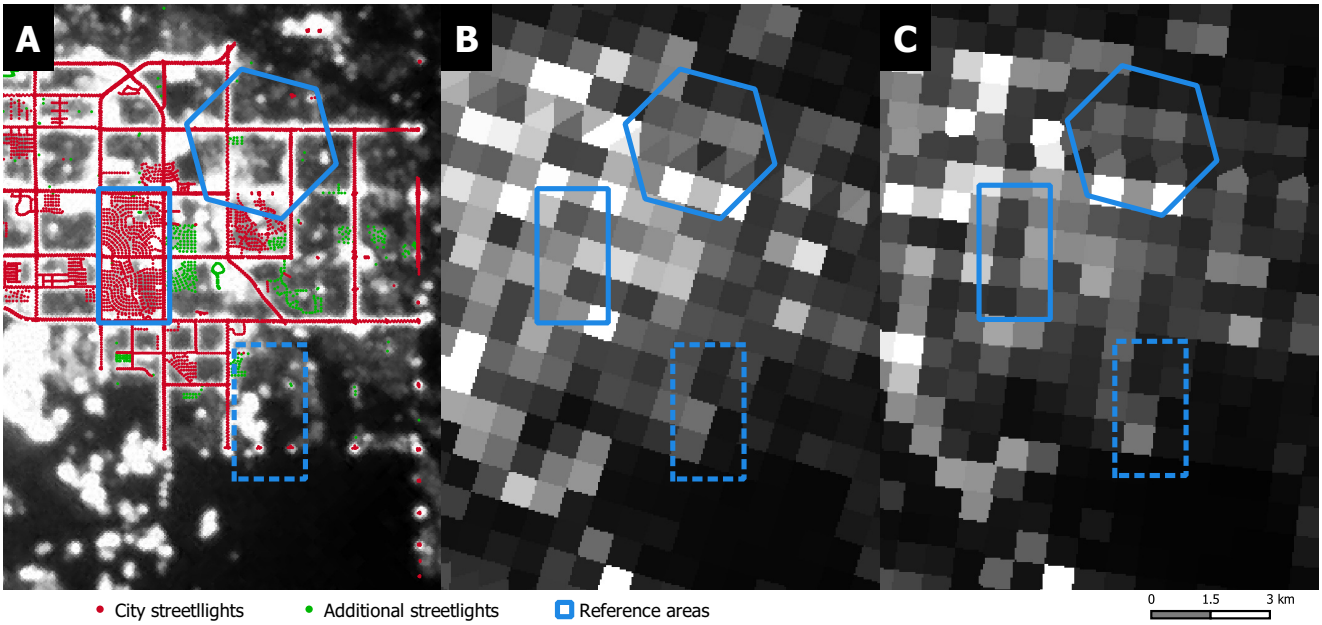

Figure 3. Zoomed in view of DNB data. The left hand frame shows a zoom in of the astronaut photograph of Tucson from 2012 shown in Fig. 12, with a focus on the eastern suburbs of Tucson. The image has been converted to grayscale, in order to make it easier to see the locations of streetlights overlaid (red and green dots). The center frame shows the same area observed by DNB on the morning of the brightest night (7 April 2019), and the right frame shows the area on one of the dim nights (31 March 2019). The orientation of the pixels changes between the two nights. The rectangular and hexagonal areas highlight certain features discussed in the main text.

the person doing an analysis chose a similarly shaped area that was shifted 200 meters westward, then 147 streetlights would be included in the rectangle. Similarly, the nightly changes in the orientation and positioning of the DNB pixels can impact which pixels contain bright private light sources, such as the area near the top left of the solid rectangle (a shopping mall parking lot). In order to reduce the impact of spatial aliasing, we created a hexagonal grid of individual analysis regions, each with 10 km^2 area. One of these hexagons is shown in Fig. 3, and the full study area is shown in Fig. 4.

To further reduce the potential for spatial aliasing, the hexagons were tilted by 15 degrees, in order to ensure there were no edges that ran in the direction of major streets (either North-South or East-West). We examined hexagonal grids with several different areas, and chose 10 km^2 for the final analysis as it offered a good compromise between substantial spatial averaging and the total number of individual hexagons in the study area. We selected hexagons for the analysis if they included City of Tucson streetlights that consumed least 4 kW of electrical power in the dimmed condition (yellow hexagons in Fig. 4). Note that at the edge of the town, the hexagons include lights or unlit areas outside of the Tucson city boundaries.

Radiance correction The DNB detects electromagnetic radiation in the spectral window 500-900 nm[26] (this overlaps but is not equivalent to "visible light" in the 400-700 nm weighted by the V_λ curve). In the DNB wavelength range, views of the Earth from space include electromagnetic radiation from both natural and artificial sources. Natural sources consist of reflected or scattered twilight, moonlight, and starlight, as well as direct and reflected atmospheric airglow and aurora, and in some cases visible and infrared light from wildfires. The experimental data were taken during a time period when there was no twilight or moonlight present, but atmospheric airglow is always present in night lights data.[27,28] Since airglow and starlight both reflect from the ground, areas with high albedos can have larger values than e.g. water bodies.[28,29] This effect is smaller on land, and is ignored here.

Airglow is variable from night to night, and the observed radiance of airglow increases with path length through the upper atmosphere (i.e. airglow radiance is larger for larger nadir angles). Our airglow correction is based on the radiance observed in hexagons that are not expected to contain artificial illumination. A complication is that artificial light emissions are scattered in the atmosphere, and therefore produce a glow around cities. This is seen as skyglow from the ground,[22,3] and as diffuse fuzz in night lights imagery[29] (often inaccurately referred to as "blooming"). For this reason, we selected a set of hexagons northeast of Tucson behind the Santa Catalina mountain range (green hexagons in Fig. 4) to correct the airglow.

Following widespread precedent in the analysis of night lights data,[30,31,32,33,34,35] we calculate a "sum of lights" (S) by adding up the radiance observed in a collection of pixels over a given analysis area. The uncorrected sum of lights $S_{h,i,\mathrm{uncor}}$ in the 50 meter raster was calculated for each hexagon h and each night i in QGIS, using the routine "raster statistics for polygons" (available in SAGA integration[36]). This routine weights pixel contributions by area, so pixels that straddle boundaries contribute proportionally to multiple hexagons. For convenience, the sum was then divided by 400 in order to set the sum of lights relative to an emission area of 1 square km:

$$\begin{aligned} S_{h,i,\mathrm{raw}} &= S_{h,i,\mathrm{uncor}}/(1000\mathrm{m}/50\mathrm{m})^2 \\ &= S_{h,i,\mathrm{uncor}}/400 \end{aligned} \tag{1}$$

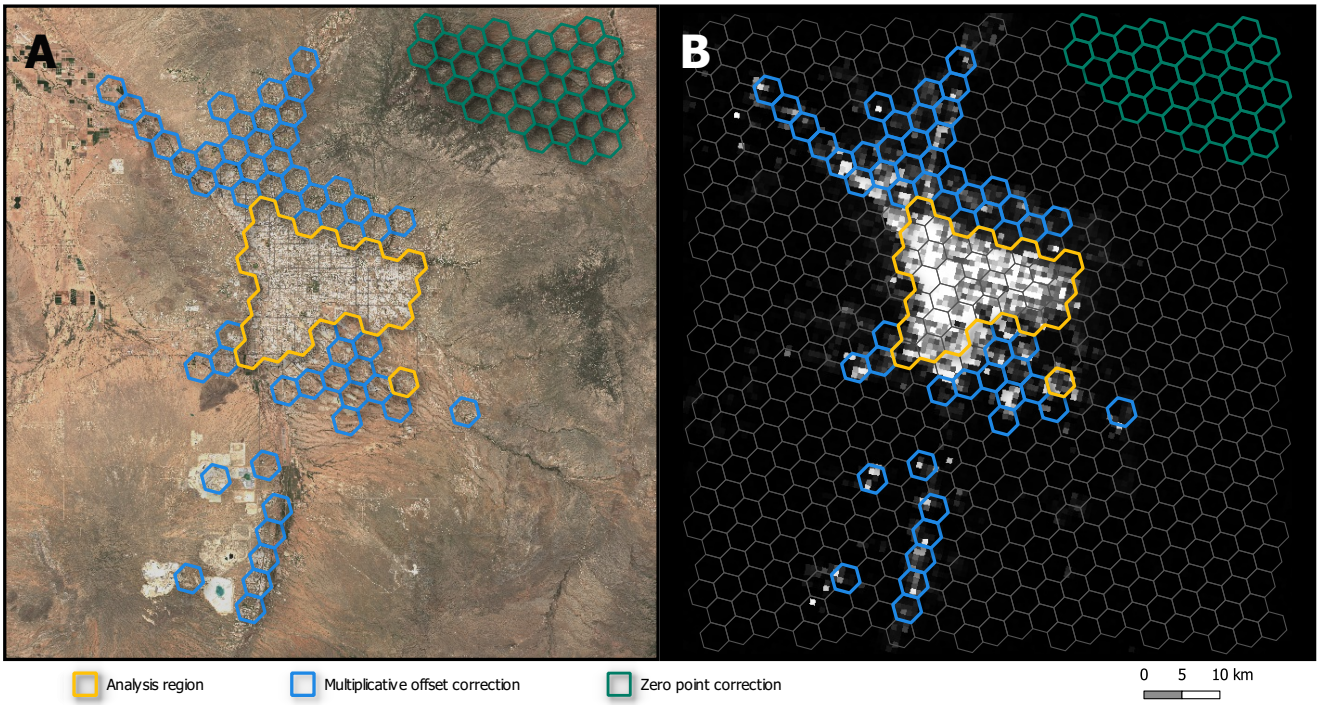

Figure 4. Tucson study area and analysis regions. The study region was overlaid with a hexagonal grid, and is shown with a background daytime image from 20 April 2019 (Panel A) and the DNB data acquired on the morning of 3 April 2019 (Panel B) (Sentinel 2 image produced from ESA remote sensing data, DNB product generation by NOAA). The three different analysis areas used in the study are color coded in both images. The green region at northeast (top right) behind the Santa Catalina mountain range is used for the zero point correction. The areas contained within the blue hexagons are used for a linear correction factor, and have an average DNB pixel radiance greater than 3 nWcm^{-2}sr^{-1}. The areas contained by the yellow hexagons are regions in which streetlights controlled by the city of Tucson consumed at least a total of 4 kW of electrical power during the dimmed condition.

Table 5. Statistical variation in the summed radiance of the hexagons used for the zero offset correction ($S_{h,i,\mathrm{raw}}$) and for the zero point corrected radiance relative to its median ($r_{h,i}$) for the hexagons used to generate the correction parameters. For each of these, the median, mean, sample standard deviation (SSD) and standard error of the mean (SEM) of the hexagons used for the correction are shown. Note that on the night of April 7, one hexagon was 60% brighter than its median. Removing it would change the median for that night to 1.086 and mean to 1.109.

Date	**Zero offset radiances**				**Multiplicative offset factors**			
	Median	Mean	SSD	SEM	Median	Mean	SSD	SEM
29 March 2019	1.75	1.73	0.13	0.02	0.961	0.967	0.094	0.013
31 March 2019	2.40	2.42	0.29	0.05	0.990	0.979	0.064	0.009
3 April 2019	2.59	2.62	0.14	0.02	0.993	0.971	0.064	0.009
7 April 2019	4.30	4.30	0.40	0.07	1.087	1.12	0.14	0.02
8 April 2019	3.02	3.03	0.17	0.03	0.989	0.993	0.086	0.012
11 April 2019	1.64	1.63	0.19	0.03	1.024	1.024	0.060	0.008

In other words, if a uniformly illuminated surface was glowing with 50 nWcm^{-2}sr^{-1}, then the sum reported for a 1 km^2 analysis area would be $S_{h,i,\mathrm{raw}}$ = 50 nWcm^{-2}sr^{-1}, and the sum for one of our 10 km^2 hexagons would be $S_{h,i,\mathrm{raw}}$ = 500 nWcm^{-2}sr^{-1}. The zero point correction factor ($S_{0,i}$) is defined as the median $S_{h,i,\mathrm{raw}}$ observed among all zero point correction hexagons (green hexagons in Fig. 4). The zero point corrected sum for each hexagon h on night i is then $S_{h,i,zp} = S_{h,i,\mathrm{raw}} - S_{0,i}$. The statistical variation among the radiance observed in the the zero point correction hexagons are given in Tab. 5.

Even after zero point correction, the radiances observed by DNB are not perfectly constant.[37] One obvious reason for this is atmospheric extinction: when the atmosphere is less transparent, artificial light sources appear less bright (although their surroundings may appear more bright due to scattering into the line of sight[29]). Atmospheric extinction changes from night to night, and total extinction along a given line of sight depends on nadir angle; at higher nadir angles light propagates through a longer path length of atmosphere, approximately as $\cos^{-1}\theta$. However, a more important reason for the changes from night to night in cities is that the Earth's night face is not a horizontal Lambertian emitter. Illuminated signs and facades, for example, are only visible from certain viewing directions, and appear brighter with increasing nadir angle.[38] In areas with tall buildings and trees, the view of the street level is partially or totally obscured. Improving understanding of the angular distribution of emissions from cities is an active field of research,[39,40,3,41,42,43,44] and remains one of the most important open questions in remote sensing of night lights and simulations of sky brightness. Finally, temporal factors also affect the radiance viewed from space. On timescales longer than this study seasonal factors become important,[45,38,14] due to changes in foliage cover and albedo (especially snow). Human factors also cause changes on several timescales. For example lights

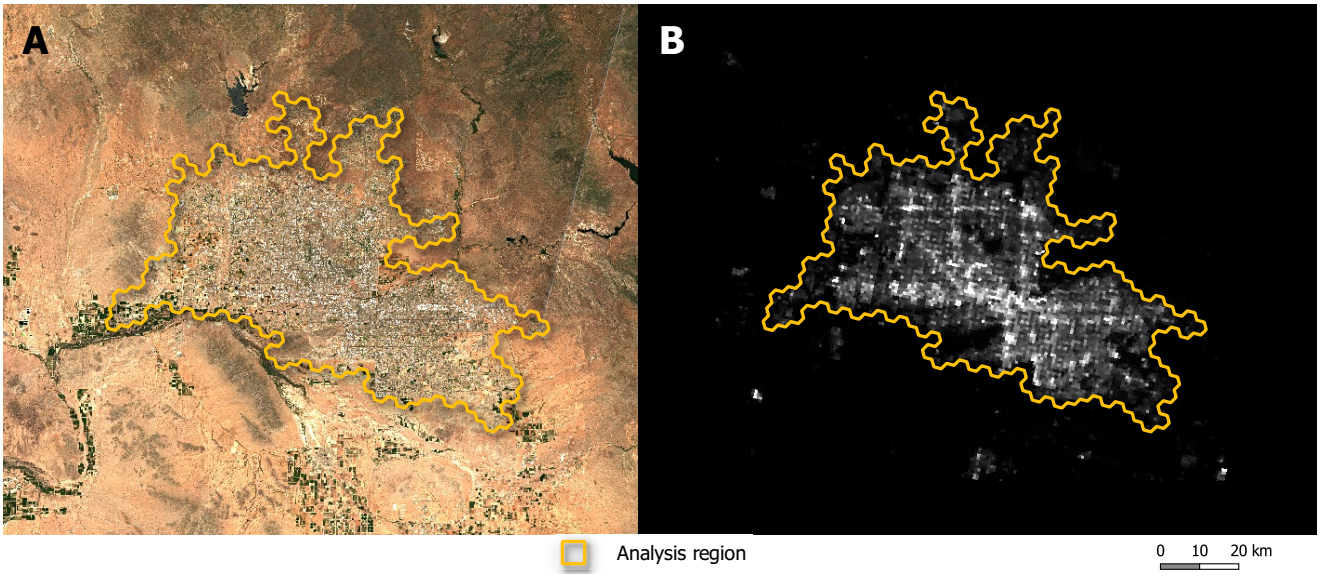

Figure 5. Phoenix study area and analysis regions. The Phoenix region was also overlaid with a hexagonal grid, shown with a background daytime image created from images taken on 18, 25, and 28 April 2019 (Panel A), and the DNB data acquired on the morning of 29 March 2019 (Panel B) (Sentinel 2 image produced from ESA remote sensing data, DNB product generation by NOAA). The areas contained by the yellow hexagons have $\tilde{S}_h > 30$ nWcm^{-2}sr^{-1}, which is the same requirement that was used for the Tucson correction.

turn off and car traffic decreases as the night progresses, and the weekend could be different from work days. These effects are discussed in a later section.

We apply a single multiplicative correction to relatively account for these factors, based on DNB radiance observations of the lights of nearby communities (which we assume to stay constant from night to night). First, for each hexagon that does not contain any streetlights operated by the City of Tucson, we found the median value ($\tilde{S}_h$) of $S_{h,i,zp}$ for the 6 nights. Hexagons with $\tilde{S}_h$ above 30 nWcm^{-2}sr^{-1} (i.e. spatially averaged DNB radiance greater than 3 nWcm^{-2}sr^{-1}) were selected as "lit hexagons" (blue hexagons in Fig. 4). We then calculated the radiance of each hexagon on each night relative to its median ($r_{h,i} = S_{h,i,zp}/\tilde{S}_h$). Next, we calculated the median value of $r_{h,i}$ among the lit hexagons for each night; these linear correction factors (g_i) are listed in Tab 4, and the statistical variation among the $r_{h,i}$ are given in Tab. 5. Finally, we applied these two correction factors to all hexagons in order to obtain a corrected sum of lights:

$$S_{h,i,cor} = (S_{h,i,raw} - S_{0,i})/g_i \quad (2)$$

In this way, if the DNB radiance observations in the communities surrounding Tucson are brighter one night for some reason, then the radiance values within Tucson are decreased correspondingly. A similar procedure using the same correction factors was applied in order to analyze the full city of Tucson. The only difference was that the zero point subtraction was based on $S_{0,i} \times (A_{\mathrm{Tucson}}/10\mathrm{km}^2)$, in order to correct the zero point for the full area of Tucson (A_{Tucson}) rather than the 10 km^2 of the hexagons.

The effectiveness of the correction is demonstrated in two ways. First, the correlation between total electrical power for street lighting and summed radiance observed became tighter once the correction is applied (see Results). Second, we examined what impact the correction had on the radiance observed for DNB radiance observations of the city of Phoenix, Arizona, on cloud free nights.

Phoenix is roughly 170 km northwest of Tucson. It is at a considerably lower elevation than Tucson (~330 m compared to ~730 m), but the two cities generally share the same large scale weather. Coesfeld et al.[38] have shown that variation over time in individual DNB pixels is correlated at short distances, but that this correlation decreases with increasing separation. We therefore expect that if the correction developed for Tucson is applied to the radiance observed for Phoenix (Fig. 5), it should at least marginally reduce the variance of the Phoenix data from night to night. Indeed, we find this to be the case: the variation from the summed radiance from the contiguous Phoenix lit region from night to night is reduced when the Tucson-based correction is applied (Fig. 6A). The variation of the radiance in each hexagon in Phoenix compared to its own mean is also reduced (Fig. 6B,C).

Stability of non-city lights and blue light emissions. Light emissions from urban areas are not constant, but tend to decrease over the course of the night,[46,47,3,20,48,49] and can differ between weekdays and weekends.[50] Under the assumption that communities surrounding Tucson have similar temporal profiles to Tucson, the multiplicative offset correction will also account for this. While emissions from a single pixel can change considerably depending on its imaging angle and exact position and orientation on Earth,[43,51,44] the sum of multiple pixels is more stable.[38] This is especially the case after our multiplicative offset correction, and when summing lights over an entire city.

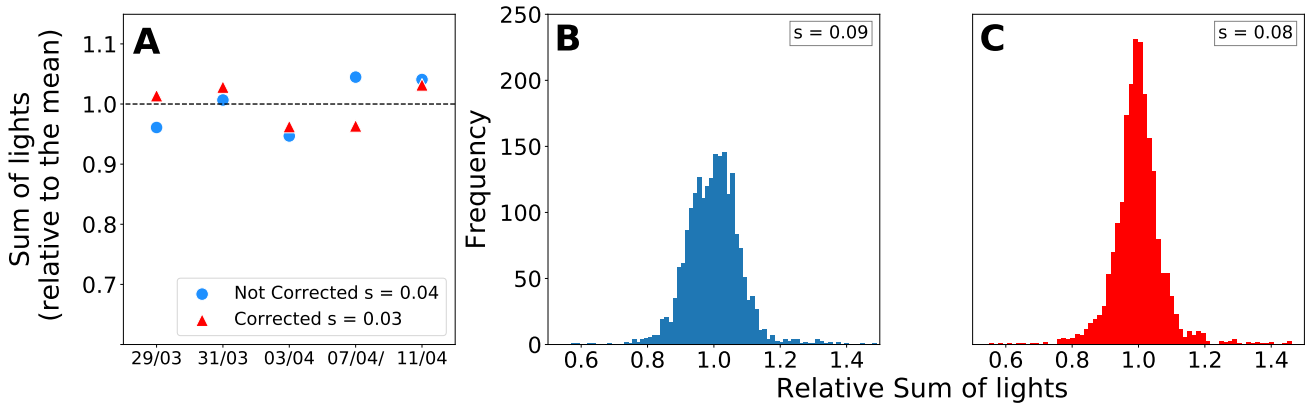

Figure 6. Impact of applying the Tucson background and multiplicative offset corrections on DNB radiance observed from Phoenix. The difference relative to the mean for the sum of all emissions from Phoenix was reduced on four of the five nights (Panel A). Compared to when not applied (Panel B), the variation from night to night among the individual hexagons was also reduced (Panel C). Here s represents the sample standard deviation.

While this experiment was taking place, we also conducted measurements of sky brightness.[52] These experiments showed that there is a consistent and substantial change in lighting at midnight, which we attribute to private lighting on timers (skyglow reduced by an estimated 2.5% due to changes in non-City of Tucson lights at midnight). Since there is not a straightforward relationship between skyglow and DNB radiance, here we report only results for the period during which DNB flies over (around 2:20 local time).

As mentioned earlier, the DNB detects electromagnetic radiation in the spectral window 500-900 nm. In contrast to human vision (∼400-700 nm), the DNB has sensitivity to an infrared emission line from high pressure sodium lights, and is blind to the "blue peak" of white LED emissions. For an equivalent lumen emission, the DNB could therefore rate a white LED as being up to 30% fainter than a high pressure sodium lamp,[2] depending on the specific spectra of each.[53] The "undercounting" of visible light is largest for cold white LEDs, and somewhat reduced for the 3000 K LEDs installed in Tucson. The DNB may have reduced or enhanced sensitivity (relative to human vision) for other light sources, such as automobile headlights and metal halide lamps, depending on their spectra.

While the spectrum of outdoor lighting is an important challenge for monitoring long-term changes, it is not particularly relevant for this analysis. This is because the spectra of Tucson's LED streetlights is the same regardless of the dimming level, and the same reduction in sensitivity occurs to a greater or lesser extent for all white light sources, including privately sources such as illuminated signs. The environmental impacts of artificial light emissions, such as sky brightness and attraction to animals, depend on both the spectra and dose. To reiterate a point from the introduction: this study does not make claims about the contribution of street lights to sky brightness or other impacts of light pollution generally, but rather aims to better understand the extent to which streetlights contribute to the radiance that satellites observe.

Percentage of streetlight emissions

It is possible to estimate how bright a region would be if all of the streetlights were turned off, by extrapolating the relationship between streetlight electrical power and observed sum of lights to zero power (Fig. 7). The fraction of total radiance observed due to the public street lighting system is $f_{\mathrm{SL}} = S_{\mathrm{SL}}/S_{\mathrm{N}}$, where S_{N} is the sum of lights when the streetlights are set to nominal power, and S_{SL} is the fit sum of lights from streetlights only. The slope of the relationship, μ_s, is a conversion factor that relates streetlight electrical power to the radiance observed from space due to streetlights. The units of this slope are $\mathrm{nWcm^{-2}sr^{-1}kW^{-1}}$. (In principle, one could cancel the nW and kW terms, and even include the total area summed ($\mathrm{km^2}$) in the numerator to further cancel out the area terms. We do not do this, because the units refer to different things (nW to the radiant power observed on a sensor in space, and kW to the elecrical power of streetlights on the ground). In addition, this would leave the slope being reported in units of 1/sr, which is far less enlightening than if the distance and power terms are simply left in place.)

We fit the data for each hexagon and for the full city of Tucson (including South Tucson) using linear regression (seaborn.regplot was used to draw the fits and 95% confidence intervals (CI), software DOI: 10.5281/zenodo.883859). The quality of the fit varied considerably from hexagon to hexagon (Figs. 8, 9). In some cases, there was a robust correlation between the observed sum of lights and the streetlight electrical power consumption. In other cases, and especially where either the total amount of streetlight power was low or there were considerable emissions from non-street lighting sources, the correlation was poorer (see Results).

As discussed earlier, not all of the streetlights in Tucson correctly reported their operating Wattage. We therefore used the nominal operating Wattage P (Tab. 1), to estimate the fraction of observed DNB radiance due to streetlights (f_{SL}) on a standard night, assuming that all of the lamps operate as intended. The fraction of light due to streetlights f_{SL} is calculated

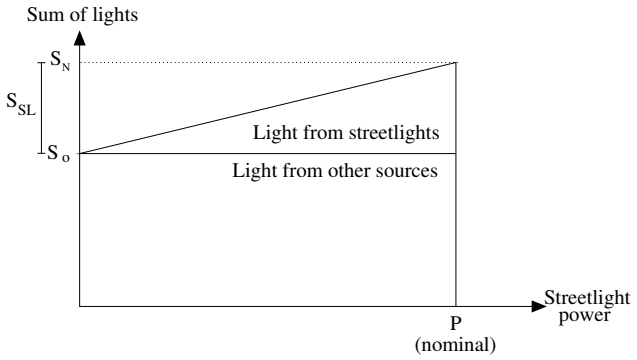

Figure 7. Relative contributions of light sources as a function of streetlight electrical power. This is a conceptual graph, and should hold for any wavelength band as long as the spectral flux of the light source is proportional to electrical power.

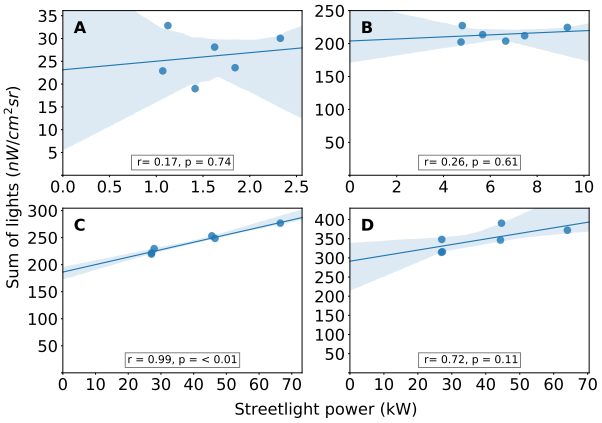

Figure 8. Relationship between streetlight electrical power and observed radiance for four selected hexagons. The positions of the four hexagons are shown in Fig. 9. Note the very different ranges in electrical power on the x-axis.

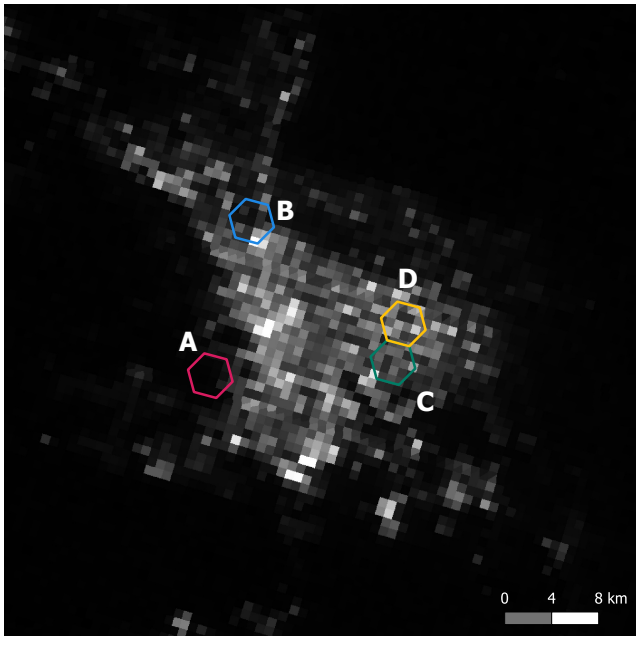

Figure 9. Location of hexagons presented in Fig. 8.

using the slope μ_s, and y-intercept (S_o):

$$f_{\mathrm{SL}} = \frac{S_{\mathrm{SL}}}{S_o} = \frac{\mu_s P}{S_o + \mu_s P} \tag{3}$$

We did the calculation with two nominal Wattages: first, the standard electrical power in Tucson between 0:00-3:00. Second, we estimated the fraction that would be due to street lighting if Tucson operated all streetlights at 100% of rated power, as

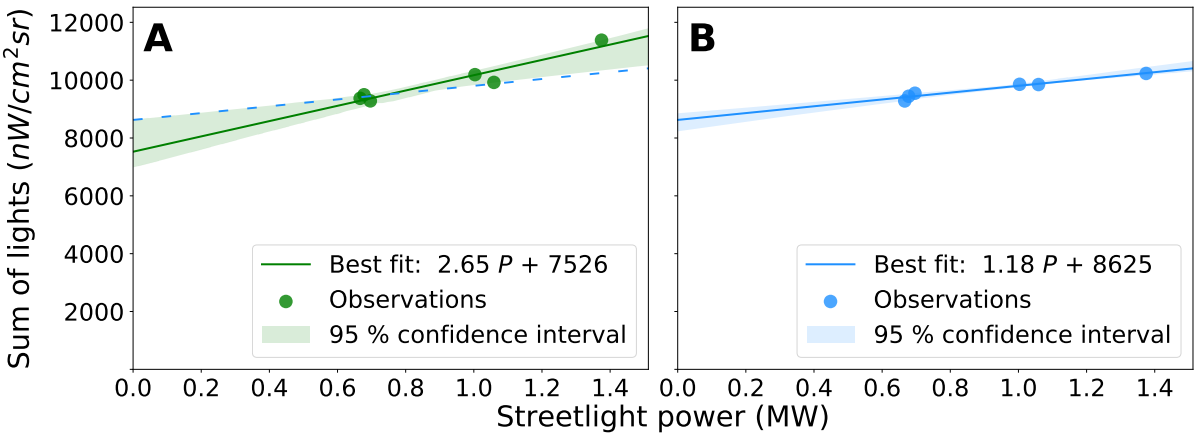

Figure 10. Comparison of corrected sum of lights and streetlight electrical power. The summed radiance within the city limits of Tucson on each night is plotted relative to the total electrical power of the City of Tucson street lighting system for uncorrected DNB radiance (A), and with zero point and multiplicative offset correction applied (B). A linear fit is shown, along with the 95% confidence interval of the fit (the dashed line in A is the fit from B). The extrapolation of the fit down to zero power shows what the radiance of the city would be if all streetlights were turned off. Note that the slope is reported in units of nWcm^{-2}sr^{-1}kW^{-1} to be consistent with the analyses of smaller areas in the Methods.

Table 6. Total streetlight electrical power and summed radiance within the Tucson city limits (including South Tucson) during the experiment. Sum of lights is in nWcm^{-2}sr^{-1} relative to a 1 km^2 area (see Methods).

Date (UTC)	Streetlight power (mW)	Raw sum of lights	Corrected sum of lights
29 March 2019	0.70	9,280	9,550
31 March 2019	0.68	9,500	9,440
3 April 2019	0.67	9,370	9,280
7 April 2019	1.38	11,400	10,200
8 April 2019	1.06	9,920	9,850
11 April 2019	1.00	10,200	9,860

most cities around the world currently do. Finally, we repeated the calculations again, this time also including streetlights not operated by the city (green dots in Fig. 2). We use the estimated electrical power consumption of the streetlights operated by non-city entities, and assumed that μ_s was the same for non-LED streetlights (μ_s=1.18 nWcm^{-2}sr^{-1}kW^{-1}). Given that they are mainly high pressure sodium lights, it is likely that their true value of μ_s is slightly different, but this assumption at least allows us to make an estimate of their contribution to the DNB radiance.

Estimating the uncertainty on the streetlight fraction and μ_s would be challenging, and would require considerably more data (e.g. to understand how the radiance from the hexagons changes from night to night when the streetlights are operating in a standard condition, and how effective the multiplicative correction is). However, it is possible to provide a rough estimate of the uncertainty based on the linear regression. Another way of expressing Equation 3 is:

$$f_{\mathrm{SL}} = \frac{S_N - S_o}{S_N} \tag{4}$$

We evaluated the value for f_{SL} using the 95% confidence interval bounds of the y-intercept, with S_N set as the value calculated with the best fit. This provides a reasonable estimate for the 95% confidence interval for the fraction of street light. However, six nights is a limited sample, and systematic uncertainties have not been taken into account.

3 Results and Discussion

We find that by making controlled changes in the light output selected sources, it is possible to determine what fraction of the radiance detected by space is due to those sources (Fig. 10). The summed radiance detected from inside of the Tucson city limits (Fig. 1, including South Tucson) is shown in Tab. 6. Using this technique, we find that streetlights controlled by the City of Tucson are responsible for 13% of the radiance observed by the DNB after midnight in the wavelength range 500-900 nm. The 95% confidence interval (based only on the statistical variation in the data) is from 10-16%.

Tucson dims most streetlights from 90% to 60% of rated power after midnight. If Tucson did not apply dimming (as is the case for most street light installations worldwide), then the public streetlights would be responsible for 18% of the total DNB radiance observed from space (95% CI 15-23%). If streetlights operated by non-city actors are included, the two best-fit values would rise to approximately 16% and 21%. All of these fractions are presumably smaller in the early evening, when more private lighting is active.[52] Determining this value for before midnight cannot be achieved without a night lights observing satellite with an earlier overpass time.

The slope of the relationship between summed radiance and streetlight electrical power (1.18 nWcm^{-2}sr^{-1}kW^{-1}, see Fig. 10) can be considered a conversion factor μ_s that allows one to predict the summed radiance S (in nWcm^{-2}sr^{-1}) that

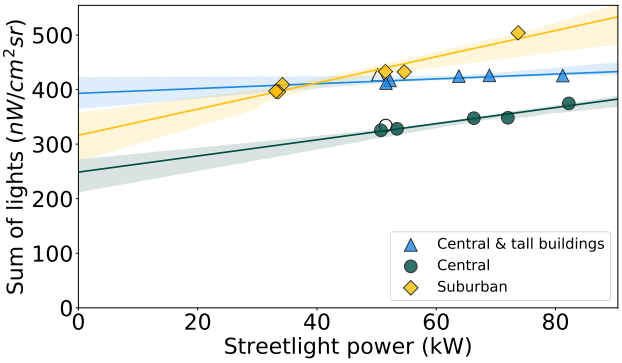

Figure 11. Relation between summed lamp electrical power consumption and summed corrected radiance in three selected areas of the city. The city center areas are each 10 km^2, while a 40 km^2 area was summed in the suburbs, in order to show similar electrical power and summed radiance (positions shown in Fig. 12B). A linear regression fit with 95% confidence interval is shown for each region. The "central & tall buildings" area includes much of the University of Arizona, which has outdoor area lighting that is not part of the city of Tucson street lighting system. The two unfilled points were not included in the fits (see Methods).

would be observed by DNB if an area of 1 km^2 was lit exclusively by Tucson-style streetlights that had a total power output of P kiloWatts ($S = \mu_s P$). It would be tempting, but incorrect, to use this factor to convert radiances observed with DNB into predictions of total power consumption for outdoor lighting in other cities, or worldwide. Consider that in cities with tall objects such as buildings or trees, the view of streetlights from space can be blocked.[22,42] Such blocking would decrease the value of μ_s, and this would invalidate the prediction in those areas. Furthermore, streetlights are responsible for only a portion of emissions, and other applications (e.g. advertising, facade lighting) have different angular and spectral emission profiles. There is no reason to believe a priori that the relation between electrical power consumption and radiance observed from space for these "other" urban light sources (i.e. μ_o) should have the same value as μ_s.

In addition to examining the city as a whole, we also subdivided the city into parcels of 10 km^2 on a hexagonal grid (hexagons reduce the impact of spatial aliasing, see Methods). At smaller spatial scales, the variation in detected radiance from night to night becomes larger. This is due to inconsistent positioning of the image pixels in different satellite acquisitions, and changes in which light sources and reflections can be seen due to the viewing geometry (see Methods, Coesfeld et al.[38] and Li et al.[43]). The correlation between emissions and observed radiance is therefore reduced compared to that observed for the whole city (Fig. 11-12). Nevertheless, it was still possible to see a relationship, provided that the change in electrical power for the city lighting during the experiment was greater than roughly 5 kW. We found that the relative contribution of streetlights to the total radiance and the best fit slope μ_s both vary throughout the city (Fig. 12).

In the regions of the city with the highest radiance, the fraction of DNB radiance due to streetlights tends to be smaller (Fig. 12B,D). To show this more directly, we calculated the Pearson correlation coefficient between the two (Fig. 13). While there is clearly a relationship (r=-0.47), radiance itself is not a particularly effective predictor for the fraction of streetlight. We also found a correlation with similar strength between μ_s and radiance (r=-0.58), which means that in bright areas a smaller fraction of streetlight emissions are detected from space. This makes intuitive sense: the brightest city center areas not only have more advertising and facade lighting, they also tend to have taller buildings than more dimly lit residential regions. In regions with tall buildings, a greater amount of the light reflecting from the street level is blocked from the DNB view.[47,38,43,14,44]

In general, the smaller the area that is analyzed, the larger the night-to-night variation of the DNB data. This is to be expected, both because of the jitter in the positioning of the DNB pixels, but also because at small distance scales, individual light sources like lit facades, billboards, and misdirected floodlights make up a larger fraction of the total light. These sources are strongly non-Lambertian, but when many of them are added together over large areas, the variation in intensity with direction reduces via a process analogous to the law of large numbers or regression towards the mean. The results presented in Fig. 12 should therefore be understood to be indicative of a trend, and not high-precision measurements of each region of the city. Similarly, the one hexagon with a negative fit slope is simply due to poor correlation in a region mainly lit by sources other than City of Tucson streetlights.

Any luminaire based on LED technology could in principle be dimmed, but with a small number of exceptions, municipalities worldwide do not use this capability. This is unfortunate, as the example of Tucson shows that dimming allows a city of half a million people to reduce its annual energy consumption by over 800 MWh per year, saving roughly $100,000/year on top of what was saved by converting from HPS to LED lights. Municipalities often purchase street lighting as a service rather than owning the streetlights themselves. In these cases, some cities that have installed and use controls to dim lights do not receive a discount in their lighting bill, because individual streetlights are not metered. The method presented here could therefore be used during the commissioning phase of a new lighting system, in order for a city to prove to the lighting provider that they are applying dimming, and justify reduced energy payments.

We originally recruited multiple cities to take part in this study (additional results are presented in the Supplemental Materials). In setting up the experiments, we learned that temporary modifications to city dimming schedules are not

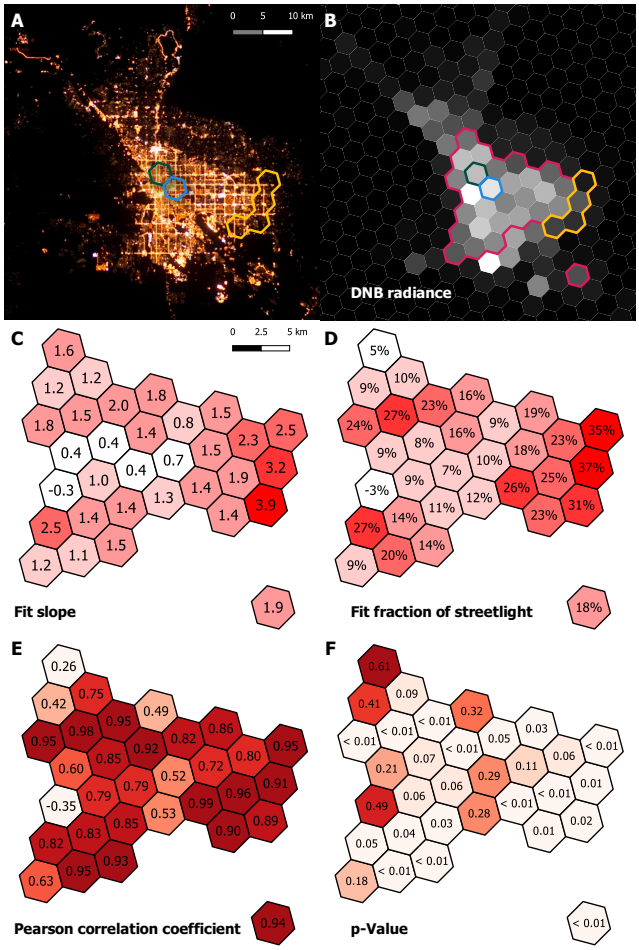

Figure 12. Variation in patterns of light emission throughout the city. (**A**) Astronaut photograph ISS030-E-183805 showing Tucson from the night of 28 March 2012 (before the citywide conversion to LED), reprojected in EPSG:32612. The yellow, green, and blue hexagons show the areas analyzed in Fig. 11. (**B**) Corrected radiance observed on the night of 8 April 2019, for which the standard city dimming schedule was applied. Hexagons inside the red outline (and including the yellow hexagons) contain at least 4 kW of streetlight electrical power consumption under the dimmed condition. (**C**) Best fit values for the relation between streetlight power and observed radiance μ_s. The spatial scale is larger than in **A** and **B**. (**D**) Fit fraction of DNB radiance due to the street light system throughout the city. (**E**) Pearson correlation coefficient r for each hexagon. (**F**) the p-value for observing such a large correlation under the assumption of no relationship.

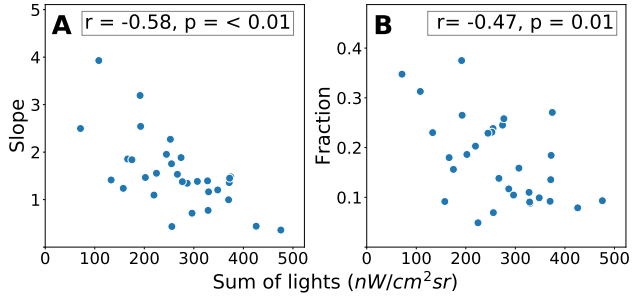

Figure 13. Relationship between radiance and best fit slope and streetlight fraction. The values for μ_s (A) and streetlight fraction (B) are plotted against the sum of lights for each Tucson study area hexagon.

straightforward. In addition, several cities discovered issues with their lighting control systems that affected their ability to control the output of their streetlights. This suggests to us that standardization in lighting control hardware and software would be beneficial. An intriguing possibility for the future would be to continually monitor the contribution of street lighting to the light emissions from a city via remote sensing. This could be accomplished by establishing a standard practice of intentional minor variations in light emission from one night to the next. For example, streetlights could be dimmed to 45% on even days of the month and 55% on odd days, or 46% on weekdays and 60% on weekends. Such a change would not be perceptible to city residents, and would be cost and energy neutral. It would, however, provide extraordinarily valuable data for research into how light emissions and total energy consumption for outdoor light are changing over the long term.[54,55,2]

4 Conclusions

This experiment demonstrates the capability of "smart city" lighting control systems to allow investigation of the makeup of urban lighting, and measurement of the relation between satellite observations and electrical power consumption for streetlights. The surprisingly small overall contribution of street lighting to total light emissions demonstrates that sustainability policy related to outdoor lighting should consider all light sources, rather than focus solely on streetlights. This is even more important for policy related to artificial night sky brightness and other forms of light pollution, as the satellite dataset used here has reduced sensitivity to horizontally emitting sources such as advertising lighting or light escaping from buildings. Reducing electricity consumption for outdoor lighting can assist the transition to a sustainable society, as it reduces the need for energy storage or non-solar electricity generation to power the lights. Lighting reductions also potentially reduce the environmental impacts of the light itself.[56,57]

This work is an important step towards the long-term goal of a method to remotely sense energy consumption for outdoor lighting. The next steps will be to gain more understanding of what light sources comprise the rest of the urban light output, and to estimate the factor μ_o that relates radiance observed from space to the energy consumption for other types of lighting. This will include, for example, examining how obstacles block upward light emissions, and quantifying how much urban light is emitted at angles too close to the horizon for satellites to observe.[39,3,58,59,42,43] A major challenge for this research will be to account for the variety in city morphology and lighting practice worldwide. As "smart city" systems become increasingly common, they will allow similar city-scale experiments to address these and other questions related to the urban environment.

Tucson does not employ the same lighting practice as other communities worldwide. Arizona has a longer history of awareness of light pollution than most places, due to the importance of professional astronomy to the state's economy. This means, for example, that some regions and cities in Arizona (including Tucson and surrounding Pima County) have ordinances regarding allowable commercial sign luminances that are not present in most localities worldwide. Tucson also hosts the headquarters of the International Dark-Sky Association, a Non-Governmental Organization that advocates for reducing light pollution. This has led to a high level of public and governmental awareness of light pollution in the Tucson area, and likely affecting lighting practice in the region (illustrated, for example, by the city's decision to considerably cut total lumen output during the conversion to LEDs). Many residential streets in Tucson do not in fact have any streetlights at all.

Compared to previous research, the results presented here for Tucson are most consistent with the estimate for the contribution of streetlight to total emissions for Flagstaff, Arizona in 2009.[15] On the other hand, the fraction of DNB emissions due to street lighting for the two German villages we examined was 28% and 42% (see Supplementary Materials), more in line with the results for Vienna[19] and Reykjavik.[18] It is well known that there are striking differences among wealthy nations when it comes to light use and per capita light emissions.[47,2,60] The extent to which these differences are due to street lighting or other types of lighting remains an open question.

The related question of the relative contribution of street lighting versus other types of lighting to skyglow also deserves further investigation. In our study of the skyglow over Tucson that was conducted together with this experiment, radiative transfer modeling suggested that street lighting was responsible for 14% of the skyglow over the city, which is similar to the result presented here for DNB radiance.[52] However, a more direct calculation based simply on the change of sky brightness at midnight in the same paper suggested street lighting is only responsible for 2-3% of the skyglow directly over the measurement locations. Our spatial results show that the fraction of light emissions due to street lights vary throughout the city (Fig. 12), and it should therefore be expected that the relative contribution of streetlights to skyglow also displays spatial variations.

Replication of these experiments in other cities is therefore highly warranted. We would be pleased to assist any large cities worldwide that wish to perform a similar experiment.

Acknowledgements

We thank the towns of Tucson, Magdeburg, Königsee, Unter-, Mittel-, and Oberköditz, Oceanside, and West Richland for their willingness to take part in both this experiment and preliminary experiments, as well as Gerolf-R. Päckert for his assistance in making contact with KD Elektroniksysteme GmbH and discussing the smaller scale experiment in Germany. CK also thanks Chris Elvidge, Kim Baugh, and the EOG team for hosting him during a visit in November 2018, and for the fruitful discussions that were a background to this work. We thank Chris Monrad for lending us a calibrated Minolta CL 200A. This research was partially funded through the European Union's Horizon 2020 research and innovation programme ERA-PLANET, grant agreement no. 689443, via the GEOEssential project. CK and HK acknowledge funding from the Helmholtz Association Initiative and Networking Fund under grant ERC-RA-0031. BE acknowledges the Road Management Office for providing lighting database information and the Sustainable Energy Authority of Ireland (SEAI) for providing financial support through its Research Development and Demonstration Fund grant 18/RDD/362.

Declaration of conflicting interests

There are no conflicts to declare.

Supplemental material

The supplementary materials document describes the methods and results of two additional related experiments that took place in Germany and Ireland. They provide further evidence of the efficacy of the method presented in the main text, and the results from Ireland show a similar relation between electrical power for streetlighting and radiance observed from space (μ_s).

References

[1] Tsao JY and Waide P. The world's appetite for light: empirical data and trends spanning three centuries and six continents. *Leukos* 2010; 6(4): 259–281.

[2] Kyba CC, Kuester T, de Miguel AS, Baugh K, Jechow A, Hölker F, Bennie J, Elvidge CD, Gaston KJ and Guanter L. Artificially lit surface of Earth at night increasing in radiance and extent. *Science Advances* 2017; 3(11): e1701528.

[3] Falchi F, Cinzano P, Duriscoe D, Kyba CC, Elvidge CD, Baugh K, Portnov BA, Rybnikova NA and Furgoni R. The new world atlas of artificial night sky brightness. *Science Advances* 2016; 2(6): e1600377.

[4] Rich C and Longcore T (eds.) *Ecological Consequences of Artificial Night Lighting*. Washington, D.C., USA: Island Press, 2006.

[5] Gaston KJ, Davies TW, Nedelec SL and Holt LA. Impacts of artificial light at night on biological timings. *Annual Review of Ecology, Evolution, and Systematics* 2017; 48: 49–68.

[6] Owens AC and Lewis SM. The impact of artificial light at night on nocturnal insects: A review and synthesis. *Ecology and Evolution* 2018; 8(22): 11337–11358.

[7] Grubisic M, Haim A, Bhusal P, Dominoni DM, Gabriel K, Jechow A, Kupprat F, Lerner A, Marchant P, Riley W, Stebelova K, van Grunsven A Roy H, Zeman M, Zubidat AE and Hölker F. Light pollution, circadian photoreception, and melatonin in vertebrates. *Sustainability* 2019; 11(22): 6400.

[8] Junker JC. Commission Regulation (EU) 2019/2020. URL https://eur-lex.europa.eu/legal-content/EN/TXT/?uri=CELEX%3A32019R2020, 2019.

[9] Kyba C, Hänel A and Hölker F. Redefining efficiency for outdoor lighting. *Energy & Environmental Science* 2014; 7(6): 1806–1809.

[10] Morgan-Taylor M. Regulating light pollution in Europe: Legal challenges and ways forward. In *Urban Lighting, Light Pollution and Society*, chapter 9. Routledge, 2015. pp. 159–176.

[11] Schulte-Römer N, Dannemann E and Meier J. *Light pollution—a global discussion*. Leipzig, Germany: Helmholtz Centre for Environmental Research GmbH, 2018.

[12] Guanglei W, Ngarambe J and Kim G. A comparative study on current outdoor lighting policies in china and korea: A step toward a sustainable nighttime environment. *Sustainability* 2019; 11(14): 3989.

[13] Zhao M, Zhou Y, Li X, Cao W, He C, Yu B, Li X, Elvidge CD, Cheng W and Zhou C. Applications of satellite remote sensing of nighttime light observations: Advances, challenges, and perspectives. *Remote Sensing* 2019; 11(17): 1971.

[14] Levin N, Kyba CC, Zhang Q, Sánchez de Miguel A, Román MO, Li X, Portnov BA, Molthan AL, Jechow A, Miller S, Wang Z, Shrestha RM and Elvidge CD. Remote sensing of night lights: A review and an outlook for the future. *Remote Sensing of Environment* 2020; 237: in press.

[15] Luginbuhl CB, Lockwood GW, Davis DR, Pick K and Selders J. From The Ground Up I: Light Pollution Sources in Flagstaff, Arizona. *Publications of the Astronomical Society of the Pacific* 2009; 121: 185–203. DOI:10.1086/597625.

[16] Kuechly HU, Kyba CCM, Ruhtz T, Lindemann C, Wolter C, Fischer J and Hölker F. Aerial survey of light pollution in Berlin, Germany, and spatial analysis of sources. *Remote Sensing of Environment* 2012; 126: 39–50.

[17] Cleaver OP. Control of coastal lighting in anti-submarine warfare. Technical report, Engineer Board Fort Belvoir VA, 1943. URL https://apps.dtic.mil/dtic/tr/fulltext/u2/a954894.pdf. Report No. 746, GN 373. Access date: 2019 May 16.

[18] Hiscocks PD and Gudmundsson S. The contribution of street lighting to light pollution. *Journal of the Royal Astronomical Society of Canada* 2010; 104: 190.

[19] Wuchterl G and Reithofer M. Licht über wien v. Technical report, Kuffner Sternwarte, 2017.

[20] Bará S, Rodríguez-Arós Á, Pérez M, Tosar B, Lima RC, Sánchez de Miguel A and Zamorano J. Estimating the relative contribution of streetlights, vehicles, and residential lighting to the urban night sky brightness. *Lighting Research & Technology* 2019; 51(7): 1092–1107.

[21] Barentine JC, Walker CE, Kocifaj M, Kundracik F, Juan A, Kanemoto J and Monrad CK. Skyglow changes over tucson, arizona, resulting from a municipal led street lighting conversion. *Journal of Quantitative Spectroscopy and Radiative Transfer* 2018; 212: 10–23.

[22] Aubé M. Physical behaviour of anthropogenic light propagation into the nocturnal environment. *Philosophical Transactions of the Royal Society of London B: Biological Sciences* 2015; 370(1667): 20140117.

[23] Longcore T, Rodríguez A, Witherington B, Penniman JF, Herf L and Herf M. Rapid assessment of lamp spectrum to quantify ecological effects of light at night. *Journal of Experimental Zoology Part A: Ecological and Integrative Physiology* 2018; 329(8-9): 511–521.

[24] Elvidge CD, Baugh KE, Kihn EA, Kroehl HW, Davis ER and Davis CW. Relation between satellite observed visible-near infrared emissions, population, economic activity and electric power consumption. *International Journal of Remote Sensing* 1997; 18(6): 1373–1379.

[25] Green J, Perkins C, Steinbach R and Edwards P. Reduced street lighting at night and health: a rapid appraisal of public views in England and Wales. *Health & Place* 2015; 34: 171–180.

[26] Miller SD, Straka W, Mills SP, Elvidge CD, Lee TF, Solbrig J, Walther A, Heidinger AK and Weiss SC. Illuminating the capabilities of the Suomi National Polar-Orbiting Partnership (NPP) Visible Infrared Imaging Radiometer Suite (VIIRS) Day/Night Band. *Remote Sensing* 2013; 5(12): 6717–6766.

[27] Noll S, Kausch W, Barden M, Jones A, Szyszka C, Kimeswenger S and Vinther J. An atmospheric radiation model for cerro paranal-i. the optical spectral range. *Astronomy & Astrophysics* 2012; 543: A92.

[28] Miller S, Mills S, Elvidge C, Lindsey D, Lee T and Hawkins J. Suomi satellite brings to light a unique frontier of nighttime environmental sensing capabilities. *Proceedings of the National Academy of Sciences* 2012; 109(39): 15706–15711.

[29] de Miguel AS, Kyba CCM, Zamorano J, Gallego J and Gaston KJ. The nature of the diffuse light near cities detected in nighttime satellite imagery. *Scientific Reports* 2020; 10: 7829.

[30] Sutton PC, Elvidge CD and Ghosh T. Estimation of gross domestic product at sub-national scales using nighttime satellite imagery. *International Journal of Ecological Economics & Statistics* 2007; 8(S07): 5–21.

[31] Elvidge CD, Ziskin D, Baugh KE, Tuttle BT, Ghosh T, Pack DW, Erwin EH and Zhizhin M. A fifteen year record of global natural gas flaring derived from satellite data. *Energies* 2009; 2(3): 595–622.

[32] Ghosh T, L Powell R, D Elvidge C, E Baugh K, C Sutton P and Anderson S. Shedding light on the global distribution of economic activity. *The Open Geography Journal* 2010; 3(1).

[33] Small C and Elvidge CD. Night on Earth: Mapping decadal changes of anthropogenic night light in Asia. *International Journal of Applied Earth Observation and Geoinformation* 2013; 22: 40–52.

[34] Coscieme L, Pulselli FM, Bastianoni S, Elvidge CD, Anderson S and Sutton PC. A thermodynamic geography: Night-time satellite imagery as a proxy measure of emergy. *Ambio* 2014; 43(7): 969–979.

[35] Li C, Li G, Tao G, Zhu Y, Wu Y, Li X and Liu J. DMSP/OLS night-time light intensity as an innovative indicator of regional sustainable development. *International Journal of Remote Sensing* 2019; 40(4): 1594–1613.

[36] Conrad O, Bechtel B, Bock M, Dietrich H, Fischer E, Gerlitz L, Wehberg J, Wichmann V and Böhner J. System for automated geoscientific analyses (SAGA) v. 2.1. 4. *Geoscientific Model Development* 2015; 8(7): 1991–2007.

[37] Ryan RE, Pagnutti M, Burch K, Leigh L, Ruggles T, Cao C, Aaron D, Blonski S and Helder D. The Terra Vega active light source: A first step in a new approach to perform nighttime absolute radiometric calibrations and early results calibrating the VIIRS DNB. *Remote Sensing* 2019; 11(6): 710.

[38] Coesfeld J, Anderson S, Baugh K, Elvidge C, Schernthanner H and Kyba C. Variation of individual location radiance in VIIRS DNB monthly composite images. *Remote Sensing* 2018; 10(12): 1964.

[39] Luginbuhl CB, Duriscoe DM, Moore CW, Richman A, Lockwood GW and Davis DR. From the Ground Up II: Sky Glow and Near-Ground Artificial Light Propagation in Flagstaff, Arizona. *Publications of the Astronomical Society of the Pacific* 2009; 121: 204–212. DOI:10.1086/597626.

[40] Kyba C, Ruhtz T, Lindemann C, Fischer J and Hölker F. Two camera system for measurement of urban uplight angular distribution. In *RADIATION PROCESSES IN THE ATMOSPHERE AND OCEAN (IRS2012): Proceedings of the International Radiation Symposium (IRC/IAMAS)*, volume 1531. AIP Publishing, pp. 568–571.

[41] Kocifaj M. Towards a comprehensive city emission function (CCEF). *Journal of Quantitative Spectroscopy and Radiative Transfer* 2018; 205: 253–266.

[42] Li X, Duarte F and Ratti C. Analyzing the obstruction effects of obstacles on light pollution caused by street lighting system in Cambridge, Massachusetts. *Environment and Planning B: Urban Analytics and City Science* 2019; : 2399808319861645.

[43] Li X, Ma R, Zhang Q, Li D, Liu S, He T and Zhao L. Anisotropic characteristic of artificial light at night–systematic investigation with VIIRS DNB multi-temporal observations. *Remote Sensing of Environment* 2019; 233: 111357.

[44] Tong KP, Kyba CC, Heygster G, Kuechly HU, Notholt J and Kollth Z. Angular distribution of upwelling artificial light in Europe as observed by Suomi–NPP satellite. *Journal of Quantitative Spectroscopy and Radiative Transfer* 2020; 249: in press.

[45] Levin N. The impact of seasonal changes on observed nighttime brightness from 2014 to 2015 monthly VIIRS DNB composites. *Remote Sensing of Environment* 2017; 193: 150–164.

[46] Lockwood G, Thompson D and Floyd R. Sky glow and outdoor lighting trends since 1976 at the Lowell Observatory. *Publications of the Astronomical Society of the Pacific* 1990; 102(650): 481.

[47] Kyba C, Garz S, Kuechly H, de Miguel AS, Zamorano J, Fischer J and Hölker F. High-resolution imagery of Earth at night: New sources, opportunities and challenges. *Remote Sensing* 2015; 7(1): 1–23.

[48] Meier JM. Temporal profiles of urban lighting: Proposal for a research design and first results from three sites in berlin. *International Journal of Sustainable Lighting* 2018; 20: 11–28.

[49] Li X, Levin N, Xie J and Li D. Monitoring hourly night-time light by an unmanned aerial vehicle and its implications to satellite remote sensing. *Remote Sensing of Environment* 2020; 247: 111942.

[50] Dobler G, Ghandehari M, Koonin SE, Nazari R, Patrinos A, Sharma MS, Tafvizi A, Vo HT and Wurtele JS. Dynamics of the urban lightscape. *Information Systems* 2015; 54: 115–126.

[51] Solbrig JE, Miller SD, Zhang J, Grasso L and Kliewer A. Assessing the stability of surface lights for use in retrievals of nocturnal atmospheric parameters. *Atmospheric Measurement Techniques* 2020; 13(1): 165–190.

[52] Barentine JC, Kundracik F, Kocifaj M, Sanders JC, Esquerdo GA, Dalton AM, Foott B, Grauer A, Tucker S and Kyba CC. Recovering the city street lighting fraction from skyglow measurements in a large-scale municipal dimming experiment. *Journal of Quantitative Spectroscopy and Radiative Transfer* 2020; : 107120.

[53] Sánchez de Miguel AS, Kyba CC, Aubé M, Zamorano J, Cardiel N, Tapia C, Bennie J and Gaston KJ. Colour remote sensing of the impact of artificial light at night (I): The potential of the International Space Station and other DSLR-based platforms. *Remote Sensing of Environment* 2019; 224: 92–103.

[54] Fouquet R and Pearson PJ. Seven centuries of energy services: The price and use of light in the United Kingdom (1300-2000). *The Energy Journal* 2006; 27: 139–177.

[55] Sánchez de Miguel A, Zamorano J, Gómez Castaño J and Pascual S. Evolution of the energy consumed by street lighting in Spain estimated with DMSP-OLS data. *Journal of Quantitative Spectroscopy and Radiative Transfer* 2014; 139: 109–117.

[56] Falchi F, Cinzano P, Elvidge C, Keith D and Haim A. Limiting the impact of light pollution on human health, environment and stellar visibility. *Journal of Environmental Management* 2011; 92: 2714–2722.

[57] Bolliger J, Hennet T, Wermelinger B, Bösch R, Pazur R, Blum S, Haller J and Obrist MK. Effects of traffic-regulated street lighting on nocturnal insect abundance and bat activity. *Basic and Applied Ecology* 2020; .

[58] Aubé M and Simoneau A. New features to the night sky radiance model illumina: Hyperspectral support, improved obstacles and cloud reflection. *Journal of Quantitative Spectroscopy and Radiative Transfer* 2018; 211: 25–34.

[59] Kocifaj M, Solano-Lamphar HA and Videen G. Night-sky radiometry can revolutionize the characterization of light-pollution sources globally. *Proceedings of the National Academy of Sciences* 2019; 116(16): 7712–7717.

[60] Falchi F, Furgoni R, Gallaway T, Rybnikova N, Portnov B, Baugh K, Cinzano P and Elvidge C. Light pollution in USA and Europe: The good, the bad and the ugly. *Journal of Environmental Management* 2019; 248: 109227.

Supplement to "Direct measurement of the contribution of street lighting to satellite observations of nighttime light emissions from urban areas"

Christopher C.M. Kyba,[1,2*] Andreas Ruby,[1,3] Helga U. Kuechly,[1] Bruce Kinzey,[4] Naomi Miller,[4] Jessie Sanders,[5] John Barentine[6,7], Ralf Kleinodt[8], Brian Espey[9]

[1]GFZ German Research Centre for Geosciences,
Telegrafenberg, 14473 Potsdam, Germany

[2]Leibniz-Institute of Freshwater Ecology and Inland Fisheries,
Müggelseedamm 310, 12587 Berlin, Germany

[3]Eberhard Karls Universität Tübingen, 72074 Tübingen, Germany

[4]Pacific Northwest National Laboratory, Portland, OR 97204, USA

[5]City of Tucson, Tucson, AZ 85701, USA

[6]International Dark-Sky Association, Tucson, AZ 85719, USA

[7]Consortium for Dark Sky Studies, University of Utah,
Salt Lake City, UT 84112, USA

[8]KD Elektroniksysteme GmbH, 39261 Zerbst, Germany

[9]Trinity College Dublin, Dublin, Ireland

[*]To whom correspondence should be addressed; E-mail: kyba@gfz-potsdam.de.

This document describes the methods and results of two additional related experiments that took place in Germany and Ireland. They provide further evidence of the efficacy of the method presented in the main text.

1 Additional experiment in Germany

A similar set of experiments was undertaken in a number of German communities at the same time as the Tucson experiment. Here we present some preliminary results to show that the method in principle also works for smaller regions. Numerous towns in Germany have opted to save energy and money not by installing LED streetlights, but by dimming their existing high pressure sodium lights. The German company KD Elektroniksysteme GmbH has developed a patented dimming system that is able to dim HPS lights without a voltage decrease that would lead to premature aging. The system is now used in hundreds of German communities each night, with a typical late-night dimming regime that results in a 67% power reduction, with a concurrent $\sim$83% reduction in lumen output measured by luxmeter.

For the mornings of April 5-9, the dimming systems were disabled in the towns of Königsee (population $\sim$2000) and the villages of Unter-, Mittel-, and Oberköditz (population $\sim$500) in Thuringia. As a result, about 300 streetlights in Königsee and about 100 streetlights in the villages increased in brightness by about 6 times during the time of the satellite overpass. Unfortunately, only one morning during the test period had clear skies in the region: 7 April 2019. We compared the results of this morning to those for 2 April and 11 April 2019, which were clear nights in which the 67% power reduction was applied as normal.

The study area is near the city of Ilmenau (location 50.6844° N, 10.9255° E, see Fig. S1). As in the Tucson analysis, we selected regions ideally containing no light emissions to do a zero point correction (green hexagons), and used nearby communities as standard candles (blue hexagons). However, because the region was smaller, we divided it into hexagons with 5 km^2 area. In addition, due to the settlement patterns in rural Germany, it is likely that the zero point regions may contain some lights (e.g. at isolated buildings). Finally, because the villages in the region are not brightly lit, the minimum average DNB radiance for the multiplicative offset correction was reduced to 2 $nWcm^{-2}sr^{-1}$ (i.e. sum of 10 $nWcm^{-2}sr^{-1}$ in the 5 km^2 hexagon).

A roughly factor 3 increase in brightness due to the dimmers being switched off is clearly observed (Fig. S1B). However, because of the non-linearity between power consumption and lumen output for dimmed HPS lights, there is not a straightforward relationship between power and observed DNB radiance. We therefore instead used the approximate relative lumen output to calculate the fraction of DNB radiance due to streetlights (Fig. S2). Caution should be taken in interpreting these results for three reasons. First, only three nights are available. Second, the lumen reduction is an estimate, based on measurements luxmeter measurements taken for an identical dimmer installation in a different city. Third, the radiance is close to the detection limit of the DNB (c.f. Fig. 8 in the main text). Nevertheless, for both communities, the best fit fraction of street lighting in the undimmed condition was still less than half of the total radiance detected by DNB: 42% for Königsee and only 28% for Köditz. (Note that since we have only 3 nights, we present best fit values only, and do not attempt to estimate a confidence interval).

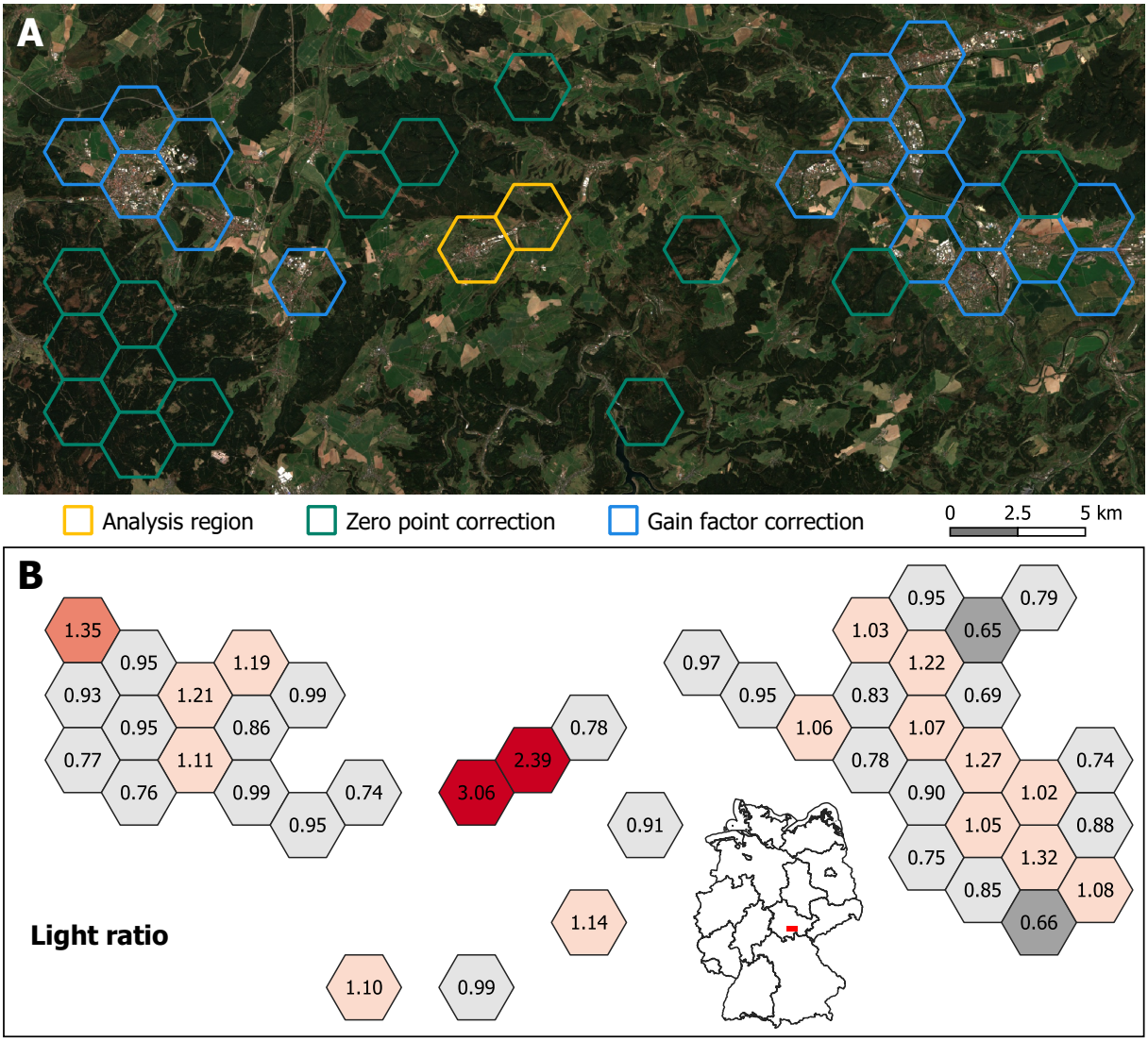

Figure S1: Germany study area and analysis regions. (A) The study region was overlaid with a hexagonal grid, and is shown with a background daytime image from 22 April 2019 (Sentinel 2 image produced from ESA remote sensing data). Green hexagons are used for the zero point correction, and blue hexagons for the multiplicative offset correction. The areas contained by the yellow hexagons are the town of Königsee (lower left) and the villages of Unter-, Mittel-, and Oberköditz (upper right). (B) The ratio of multiplicative offset corrected radiance on 7 April is compared to the mean of the other two nights for all hexagons in the region with an average radiance greater than 0.2 $\mathrm{nWcm^{-2}sr^{-1}}$ (sum greater than 1 $\mathrm{nWcm^{-2}sr^{-1}}$). The location in Germany is shown in the inset, Ilmenau is the city at upper left.

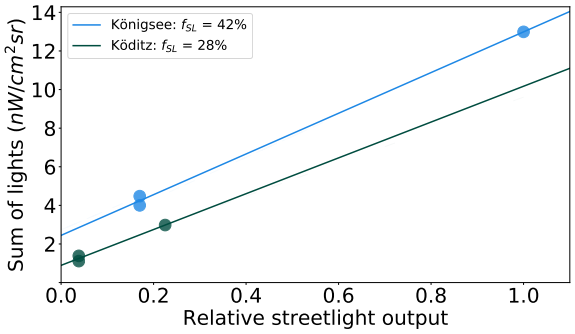

Figure S2: Relationship between summed satellite radiance and relative luminous flux output of the streetlight system for selected German towns. The radiance is plotted relative to the "nominal" streetlight luminous flux of Königsee. Königsee (lower left hexagon in Fig. S1) is shown in blue, and the combined light output of the villages of Unter-, Mittel-, and Oberköditz in Green. The streetlight luminous flux for the villages of Unter-, Mittel-, and Oberköditz is scaled relative to Königsee based on the power consumption of each when dimming is not applied. The estimated fraction of light from streetlights (s) is shown directly on the plot.

2 Additional experiment in Ireland

The methods and analyses presented above were designed for large areas which include both streetlights and other sources of lighting. In the case of an isolated area that contains predominantly one type of light source, the relationship between power consumption and light emissions can be measured more straightforwardly. We are currently working on an analysis of public street lighting in and near small communities in Ireland, and this section we present a single site case study as a "sanity check" for the slope μ_s measured in Tucson.

Ireland has recently begun a conversion to LED technology for both environmental and economic reasons. Based on data supplied by the national Road Management Office, LED luminaires now make up roughly 16% of the total power consumption reported in Ireland's public lighting database. We selected a region near the town of Mucklagh (County Offaly), which has a considerable number of high wattage LED streetlights (maximum 178 W), and little or no other lighting (Fig. S3). The town has a population of 830 people, and the analysis area contains LED streetlights that draw a total of 5.5 kW in an area of slightly larger than one square kilometer.

For this analysis, we used the composite DNB image for the month of November, 2018, produced by the Earth Observation Group (available from `https://eogdata.mines.edu/download_dnb_composites.html`). This image is based on 8-10 overpasses of the satellite during nights with clear skies and no moonlight. Scaled relative to one square kilometer (as in the main paper), and with background light subtracted, we found $\mu_s = 1.00$ nWcm^{-2}sr^{-1}kW^{-1}. This is in rather close agreement with the $\mu_s = 1.18$ nWcm^{-2}sr^{-1}kW^{-1} found for the average in Tucson, and is well inside the range of best fit μ_s shown in Fig. **??**.

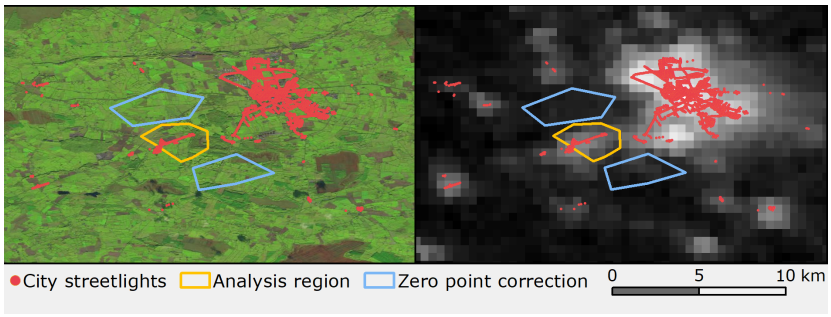

Figure S3: Irish study area and analysis regions. The study region is shown with a background daytime image from 28 October 2018 (Panel A) and the DNB composite image for November 2018 (Panel B). (Sentinel 2 image produced from ESA remote sensing data, DNB product generation by NOAA EOG.) The area inside of the yellow polygon is the study area, the areas enclosed by the two green polygons were used for background subtraction. The red dots indicate the location of street lights. The town of Mucklagh was divided, because while the northeastern side has LEDs, the southwestern side contains 55W low pressure sodium vapour streetlights. The nearby town at upper right is Tullamore, population 11,444.

Since the settlement patterns and vegetation differ so dramatically between Ireland and Arizona, this result is encouraging for the prospect of studying energy consumption for lighting on global scales.

In our forthcoming analysis, we intend to establish the relationship μ_s for a number of different types of lamps that are in common use in Ireland, and apply these values in regions where public and private lighting are mixed. This will in principle allow us to determine the ratio of public to private lighting in both rural and urban areas, although care must be taken regarding the potential for vegetation or buildings to block light at larger off-nadir angles.